

Molecular dynamics simulation of interaction between bio-molecules and metal-organic frameworks for efficient gene delivery at the nanoscale

Anahita Bakhshandeh, Fatemeh Ardestani* and Hamid Reza Ghorbani

Department of Chemical Engineering, Qaemshahr Branch, Islamic Azad University, Qaemshahr, Iran

Received: August 2022; Revised: September 2022; Accepted: October 2022

Abstract: To fabricate functional surfaces structures for protein immobilization without losing biological activity, the interaction between different amino acids and metal-organic frameworks (MOFs) has been evaluated. The density functional theory (DFT-D2) calculations were used to afford a molecular description of the interaction properties of the amino acids and MOF-5 by examining the interaction energy and the electronic structure of the amino acid/MOF complexes. Strong interactions were recorded between the amino acids and MOF through their polar groups as well as aromatic rings in the gas phase. Based on the results, water molecules prevent the amino acids from approaching the active sites of MOF, causing weak attractions between them. The interaction energies were calculated by considering the basis set superposition error correction. The interaction energies obtained at the range of +11 to -13 kcal/mol, for GLY-MOF in the presence of water molecules while in the case of the gas phase the estimated values range from -5 to -57 kcal/mol. Results showed GLY molecules cannot form a stable complex in the water media. The complication of all selected AAs is found exothermic process and energetically favorable and thus can form stable complexes with the MOF-5 at the gas phase. The accuracy of the DFT-PBE model was validated against the comprehensive MP2 quantum level of theory. The evaluation of the nature of the interaction between the amino acids and MOF by the atoms-in-molecules (AIM) theory showed that the electrostatic attractions are the main force contributing to bond formation between the interacting entities.

Keywords: Amino acids, DFT, Functionalization, MOFs, Nanotechnology.

Introduction

The increasing count of new compositions and structures along with the significant efforts being made to develop novel/optimized functionalities have contributed to the rapid growth of the knowledge on hybrid ordered porous materials during the last decade [1]. Numerous research works have been performed on metal-organic frameworks (MOFs) and their wide spectrum of potential applications in, for example, energy and gas storage, catalysis, chemical sense, medicine, drug delivery, molecular magnetism, and the development of tunable-pore size material [2-3]. The term MOF refers to the art of engineering chemical structures by combining organic and inorganic chemistry, which are commonly recognized as disparate fields.

As an emerging class of MOF, nano-sized MOFs offer a combination of intrinsic characteristics of porous materials together with the advantages of nanostructures, making them able to enhance the functionality of classical bulk crystalline MOFs [3-5]. Focusing on biomedicine, MOF miniaturization is known to be effectively advantageous based on its large contribution to administration route selection as well as governing in vivo fate and hence the drug toxicity and/or activity [4-6]. MOFs exhibit a three-dimensional (3-D) periodic structure where inorganic secondary building units are cross-linked by organic ligands. As of present, it has been shown that the MOFs enjoy some regular tunable porosity with large loading capacities; moreover, the organic linker has been also found to be well-tunable, so that it can be used to adjust interactions with particular amino acids [7-8]. As a superior benefit,

*Corresponding author. E-mail: Ardestani_fatemeh@yahoo.com
Tel: +98-1142155025, Fax: +98-1142240091

MOFs can serve as endogenous linkers. In an ideal case, this property makes the MOFs the perfect choice for bio-applications where it is highly desired to have a linker that can be reused after in-body administration, thereby strongly lowering the risk of adverse effects [3, 8]. As of current, many endogenous linker-based MOFs have been presented [9], such as the iron (III) gallate, fumarate or muconate MOF that exhibit either a rigid small-pore structure, or a highly flexible porous matrix [10]. At the other end of the spectrum, exogenous linker-based MOFs have been used as functionalized linkers for tuning the absorption, distribution, metabolism, and excretion (ADME) cycle. Moreover, when it comes to the adsorption and delivery of therapeutic molecules, the existence of functional groups within the framework can contribute to the modulation of the host-guest interactions, which enhances the control of the drug release [11]. The most popular functionalized systems of this type include iron/zinc-based porous metal terephthalates, while there have been also reporting on porous MOFs synthesized based on modified linkers with polar or nonpolar functional groups such as amino, nitrous, brooms, carboxylates, methyls, and perfluoro [12]. As building blocks of proteins, amino acids can characterize typical chemical properties of complex biomolecules [13]. Given the large part taken by proteins in different fields of application, such as medicine and nutrition, one may think of addressing crucial problems in biomedicine by thoroughly understanding amino acid-nanomaterials interactions. For instance, a study on the mechanisms through which biomolecules (e.g. proteins) are adsorbed on a synthetic surface may provide useful information on the roots of the body's response to external biomaterial implants [14-18].

Being widely available, inexpensive, and non-toxic, natural amino acids may be seen as ideal enantiopure linkers for the synthesis of homochiral MOFs [19, 20]. As a powerful tool for addressing the difficult problems encountered in this scope, molecular simulations are drawing increasing deals of attention because of the very useful insights they provide into structural dimensions and electronic characteristics of molecular systems. Recently, theoretical studies have been undertaken based on various theoretical foundations ranging from density functional theory (DFT) to molecular mechanics and further to the atomic orbital-based Hartree-Fock plus second-order Moller-Plesset (MP2) perturbation theory [21-23]. Zhang et al. suggested that, as far as the chiral

recognition ability is concerned, the MOFs whose framework contained some amino acid serving as a bridging ligand outperformed the MOFs where then amino acid ligands acted as the metal centers. In the meantime, the synthesis of the chiral MOFs using amino acid as a bridging ligand presented large potentials for HPLC separation applications [20]. In this work, interactions between the MOF-5 and the glycine (Gly) amino acid (and its tripeptide counterparts), as a simple biomolecule, were investigated using the DFT calculations. Interaction energy, electronic structure, and nature of the encountered interactions were analyzed in an aqueous medium. The long-range dispersion corrections were also considered for the interacting systems. Our first-principles findings demonstrated strong interactions between the glycine/tripeptide amino acid and MOF-5, promising potential applications of MOFs in the pharmaceutical industry.

Results and discussion

To investigate the interaction between glycine, as a non-ionic amino acid, and the MOF-5, various interaction configurations were considered. To generate initial configurations, optimized amino acid, and MOF-5 structures were used, taking into consideration the fact that the partially negatively charged atoms (e.g. nitrogen and oxygen atoms) were located in the vicinity of partially positively charged atoms (e.g. zinc atom). The initial structures were taken as input for structural optimization, followed by evaluating the interaction energies. Optimization was performed based on the revPBE-D3 model with the def2-SVP basis set. At the next step, interaction energy was calculated for interacting entities considering the BSSE correction with the def2-TZVP basis set. To investigate the interactive nature of the systems under study, the charge and electronic structure analyses were performed.

Figure 1 shows the optimized structure of the MOF-5 along with the bond lengths and angles. Considering the structure obtained using the DFT calculations, an acceptable agreement was observed between the experimental data [45] and the computational results as far as the bond lengths and angles were concerned, indicating acceptable reliability of the computational approach followed in this work. Glycine amino acid was also optimized with its structural geometry represented in the figure.

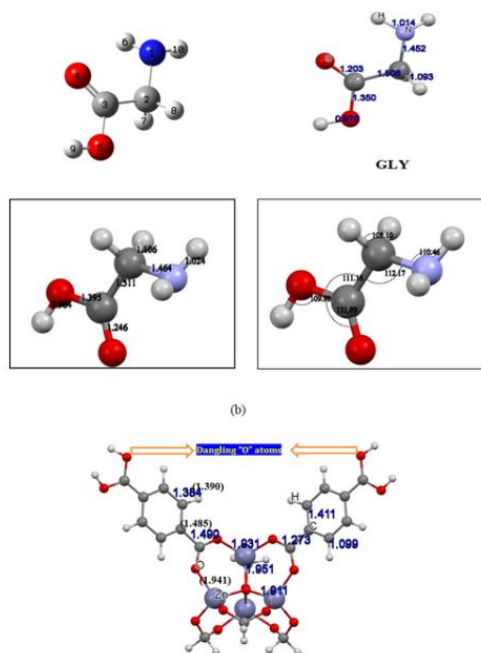


Figure 1. Optimized structures of (a) MOF-5 and (b) glycine amino acids in the aqueous phase obtained with revPBE-D3/SVP model of theory. Schematic representation of various orientations of glycine molecule approaching the MOF-5 skeleton through its different active sites. (Red: O, Gray: C, Indigo: Zn, Blue: N, and White: H)

Structural and energy properties of Gly/MOF-5:

In this section, optimized structures of glycine and MOF-5 were used to model initial configurations, followed by optimizing these molecular systems in the aqueous phase. Figure 2 represents the different configurations considered for the glycine-MOF-5 interactions.

Considering the orientation of active sites, four configurations were considered herein, as follow:

1. Gly-MOF (I): glycine molecule approaches the O atoms of the framework through its NH₂ end, while the CH group on glycine approaches the framework ring.
2. Gly-MOF (II): NH and OH groups on glycine approach the O atoms of the framework.
3. Gly-MOF (III): N atom of glycine approaches the Zn atoms of the framework, while O atom of the glycine approaches the other Zn atom of the framework.
4. Gly-MOF (IV): OH and CH groups on the glycine

approach the Zn and the O atoms of the framework, respectively. In the next stage, the modeled structure was fully optimized, and then, considering the BSSE correction, the interaction energies of the considered systems were calculated, so that the most stable configuration could be identified. Table 1 reports the calculated interaction energy (E_{ads}) of the Gly-MOF system in different configurations. Comparing the interaction energies of the four configurations considered in this work, the Gly-MOF (III) system was found to be the most stable structure based on the interaction energy (*i.e.* associated with the highest interaction energy).

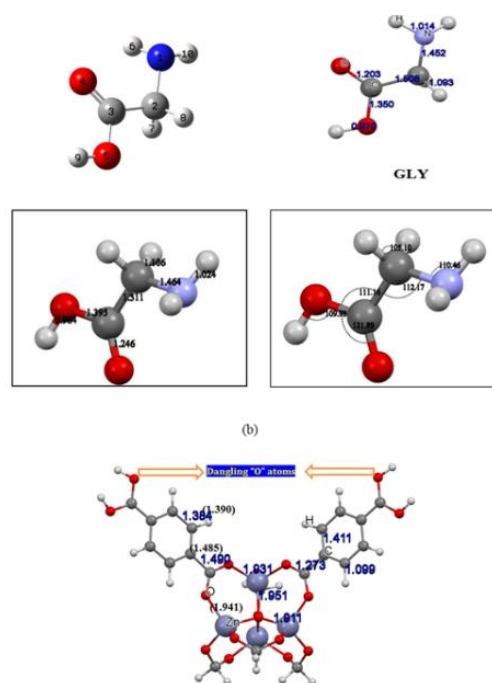


Figure 2. Schematic representation of (a) optimized structure of most stable configuration of glycine/MOF-5 and (b) selected part of optimized complex for MP2/revPBE calculation. Calculated (c) HOMO/LUMO orbitals, (d) total charge density and (e) bonding critical point (BCP) for most stable configuration of glycine/MOF-5. (The iso-values were set to 0.02 and 0.07 a.u. for HOMO/LUMO and TDens, respectively. Red and green colors denote the negative and positive signs of the Wavefunction).

Table 1. Values of interaction energies and Mulliken/Hirshfeld charge analysis for glycine amino acid/MOF-5 systems

System		E_{int} (kcal/mol)	QT (e)
Glycine			
(I)	NH ₂ -O-O-CH-Ring	0.348-	0.076
(II)	NH-O-OH-O	0.339-	0.011
(III)	-N-O-Zn-Zn	-2.935	0.432
(IV)	OH-Zn-CH-O	0.593-	0.019

System	E_{int} (kcal/mol)	E_{int} (eV)	QT (e)	D_{A-S} (Å)	Dispersion forces (kcal/mol)
Gly/MOF (water)	11.234	0.487	0.088	2.748930	-75.966
Glyc/MOF (Gas)	-5.690	-0.247	-0.135	2.268	-75.823

The DFT-D estimated values for interaction energies (E_{int}), charge transfer (QT), equilibrium distances ($DA-S$), and dispersion forces for AAs/MOF-5 system (Table 1).

Figure 2(e) shows the final equilibrium structure of the most stable Gly/MOF-5 complex, with bond lengths mentioned in the figure. According to the results, interaction energy for the energetically preferred configuration was -2.775 eV (-64.002 kcal/mol), and the equilibrium distance between the closest atom of the glycine molecule and MOF-5 (N atom of glycine and Zn atom of the framework) was about 2.099 Å. An investigation into the geometrical parameters of the glycine molecule indicated that the lengths of the N-H and C=O bonds in the geometrical structure of the glycine molecule changed from 1.464 and 1.246 Å to 1.485 and 1.251 Å, respectively. To evaluate the accuracy of the current revPBE-D3 method, a comparative analysis was performed through MP2, as a high-level quantum chemistry method, on the most stable Gly/MOF-5 configuration. To simplify the calculations, a segment of the complex consisting of the interaction regions of Gly/MOF-5 was considered, as depicted in Fig. 2(b). The single point calculations with MP2/TZVP showed an interaction energy of -1.891 eV (-43.616 kcal/mol). For exact comparison, calculations were also performed with the

DFTrevPBE/TZVP, and the interaction energy was found about -1.905 eV (-43.939 kcal/mol). A comparison between the obtained values of interaction energy indicated the validity of the implemented DFT-based method for explaining the glycine-MOF interactions.

Electronic structure and molecular properties:

To evaluate the binding nature of the amino acids attached to MOF-5, the electronic characteristics of the system were analyzed. These included the charge transfer and the molecular states as well as the molecular descriptors for the interacting entities. All calculations were performed by the revPBE-D3/TZVP model. Charge analysis by the Hirshfeld approach (as a valuable method compared to the basis set-dependent Mulliken approach [46, 47]) showed significant charge transfer from the glycine amino acid to the MOF-5 (0.465 e), indicating strong interactions between the two molecules. The calculated HOMO and the LUMO orbitals for the complex, as represented in Figure 2(c), show that the majority of the HOMO orbitals were located on the glycine molecules while most of the LUMO orbitals were on the MOF skeleton. This finding was in line with the results of charge transfer analysis where electrons were transferred from the glycine to the MOF moiety. To evaluate the nature of the interactions involved by the complex, total charge

density was computed using the revPBE-D3/TZVP model. The results demonstrated a lack of charge accumulation in the interaction region of the attached glycine to the MOF-5 but a rather minor charge accommodation between N and Zn atoms, see Figure 2(d). To gain a deeper insight into the binding nature of the Gly/MOF-5 complex, the state-of-the-art AIM analysis was also performed in this study. For this purpose, an analysis of the electronic charge density ($\rho(r)$) and its Laplacian ($\nabla^2\rho(r)$) was carried out. Based on the AIM theory, a negative Laplacian together with a negative energy density usually reveal a pure covalent bond, while positive values for the Laplacian and the energy density represent pure closed-shell

bonds (e.g. strong hydrogen bonds and ionic bonds). In the meantime, a positive Laplacian coupled with a negative energy density demonstrates an intermediated situation, i.e. highly polar and partially covalent bonds. Nevertheless, it is worth mentioning that there are also exceptions to the abovementioned laws so the type of bonds shall be identified based on not only the stated criteria but also other analyses. Figure 2(e) demonstrates the optimized structure of the Gly/MOF-5 complex accompanied by the BCPs in orange color. The calculated Laplacian and energy densities are given in Table 2.

Table 2. Calculated Laplacian and energy densities at revPBE-TZVP level of theory for energetically favorable glycine/MOF-5 complex.

(a)

	BCP1 (Zn...N)	BCP2 (N-H...O)	BCP3 (Zn...O)	BCP4 (Zn-O)	BCP5 (C-O)	BCP6 (C-H)	BCP7 (C-C)
$\rho(r)$	0.014	0.028	0.010	0.099	0.357	0.269	0.269
$\nabla^2\rho(r)$	0.041	0.125	0.042	0.522	-0.673	-0.897	-0.712
$H(r)$	0.001	0.002	0.002	-0.023	-0.605	-0.259	-0.245
$G(r)$	0.010	0.029	0.009	0.154	0.437	0.035	0.066
$V(r)$	-0.010	-0.026	-0.007	-0.177	-1.043	-0.294	-0.311

From the obtained BCP results, it can be found that there is an evident feature in the bonding region of nitrogen and Zn atom with the $\nabla^2\rho$ value of 0.307, indicating a strong charge depletion at this critical point. The calculated value of $H(rBCP)$ (-0.005 a.u) reveals the existence of an attractive interaction between the two adjacent nuclei. According to the obtained values, one can conclude that this bond has a highly polar nature comparable to the situation for ionic and coordination bonds. This is exactly in line with the findings of charge transfer analysis that demonstrated that some 0.465 e was transferred from the glycine to the MOF-5 and also the situation of the HOMO and the LUMO orbitals, as discussed previously. This finding can be attributed to the fact that the lone pair of the N atom donates electrons to the LUMO orbital of the Zn atom of the framework, resembling a coordination bond instead of a regular covalent bond. As a consequence, the strong interaction between the glycine amino acid and the

MOF-5 indicates that the Gly/MOF-5 complex is energetically stable in the aqueous phase. In the case of the O atom of the glycine interacting with the Zn atom, however, the calculated $\nabla^2\rho$ was relatively small (0.066), showing a weak depletion of charge at the corresponding critical point. Meanwhile, the magnitude of $H(rBCP)$ (-0.004 a.u) shows attractive interactions between the neighboring nuclei, and the calculated $H(rBCP)$ and $\nabla^2\rho$ parameters are positive for the Zn-O bond in the MOF, highlighting pure closed-shell bonds such as ionic bond rather than either partially covalent or highly polar bonds. Further, the corresponding parameters of the C-C bond in the glycine indicate the existence of a covalent bond with negative values of $H(rBCP)$ and $\nabla^2\rho$ (-0.172 and -0.413 a.u., respectively). Molecular properties of the considered systems (i.e. gap energy (E_g), hardness (η), and softness (s)) were reportedly closely related to the HOMO and the LUMO energy levels [48-51]. The wider the gap between the LUMO and the HOMO

orbitals, the harder and less chemically reactive would be the species. With decreasing and increasing the hardness and the softness, respectively, the reactivity increased. Therefore, the softer a species, the more reactive it would be. The calculated values of molecular properties (Table 3) demonstrated that, through the process of functionalization, the glycine amino acid has become softer and the gap energy decreased, indicating increased reactivity of the amino acid upon complexation. As a result, a higher reactivity of the complex could enhance the loading process of the amino acid in, for instance, drug delivery applications.

Effect of solvent and dispersion forces:

Table 3. Molecular descriptor parameters for glycine amino acid and glycine/MOF-5 (III) complex calculated at the revPBE-TZVP model.

	Glycine and MOF-5	Glycine
E_{HOMO} (eV)	-6.417	5.319-
E_{LUMO} (eV)	3.333-	1.618-
η (eV)	1.541	1.850
S (eV)	0.324	0.270
Gap Energy(eV)	3.083	3.701

In addition, the solvation energy could be estimated from the total energy of the Gly/MOF system in the aqueous and the gaseous phases ($E_{\text{solv}} = E_{\text{tot}}(\text{aq.}) - E_{\text{tot}}(\text{Gas})$). The solvation energy of the Gly/MOF-5 complex was determined to be about -3.760 eV (-86.696 kcal/mol), which revealed the relevant solubility of functionalized MOF-5 with glycine. Considering the importance of the long-range non-local interactions such as vdW forces in the interactions among molecular species [52-54], the effect of this factor on the interactions between the glycine and the MOF-5 was also evaluated. For this purpose, the most stable structure was subjected to optimization in absence of the corrections related to the vdW forces. Then, the BSSE of wave functions was taken into consideration for the interaction energy computation. In this case, glycine was found to react with MOF-5 at an energy equivalent of -1.984 eV (-45.751 kcal/mol). Comparing this value to that of the system examined in the presence of vdW forces showed very large differences; *i.e.* the effect of vdW force on the glycine/MOF-5 interactions was significant. It was also found that the equilibrium

In this section, to investigate the effect of solvent on the interaction of Gly with MOF-5, an optimization process was undertaken for the most stable structure in the gaseous phase. Next, the interaction energy was calculated considering the BSSE correction. The interaction energy computations revealed that, in the gaseous phase, the glycine molecules interact with the MOF-5 to release -2.070 eV (-47.734 kcal/mol) of energy at an equilibrium distance of 2.157 Å between the glycine and the MOF-5. Comparing the interaction energies in the aqueous and the gaseous phases, it was found that the solvent affected the interaction energy between the glycine and MOF-5 remarkably though the bonding nature was still strong and typical for the chemisorption.

distance between the glycine and the MOF-5 (N and Zn atoms) changed slightly from 2.099 Å in presence of vdW forces to 2.125 Å in absence of such forces. It should be noted that the interaction properties, interaction energy, and bonding distances were still typical for the chemisorption and that the lack of dispersion forces might give results far away from the real observation.

Tripeptide/MOF-5 system:

To rationalize the behavior of the proteins interacting with the MOF-5, a larger biological system was also considered: a tripeptide model of the glycine amino acid involving the zwitterionic isomer of glycine, as depicted in Figure 3(a). The interactions of the tripeptide with the MOF-5 were then evaluated to obtain further realistic results. Geometrical optimization of the tripeptide glycine structure upon the interaction with the MOF-5 demonstrated a strong deformation in the tripeptide structure together with the formation of bonds between the oxygen atoms of both carbonyl and carboxyl groups on the tripeptide and the neighboring Zn atoms, see Fig. 3(b). The adsorption led to the release of -3.661 eV (-84.423

kcal/mol) of energy, which was high enough to acknowledge the complex as stable. Performing a charge analysis based on the Hirshfeld approach, it was clear that some 0.495 e charge was transferred from the tripeptide to the MOF-5 throughout the adsorption process, indicating strong interaction of the system under investigation. The geometrical parameters of the adsorbed tripeptide further verified the above findings regarding the nature of the interactions this was based on the length of the formed O–Zn bond (~ 2.0 Å) that was a typical bond for the Zn–O bond in the zinc-oxide compounds [55]. In addition, the changes in the C=O bond length and structural deformations of the involved molecules indicated strong interactions between the tripeptide and the MOF-5. Altogether, these findings highlight the MOF-5 is a suitable material with large biological potentials that can be chemically modified for drug delivery technology.

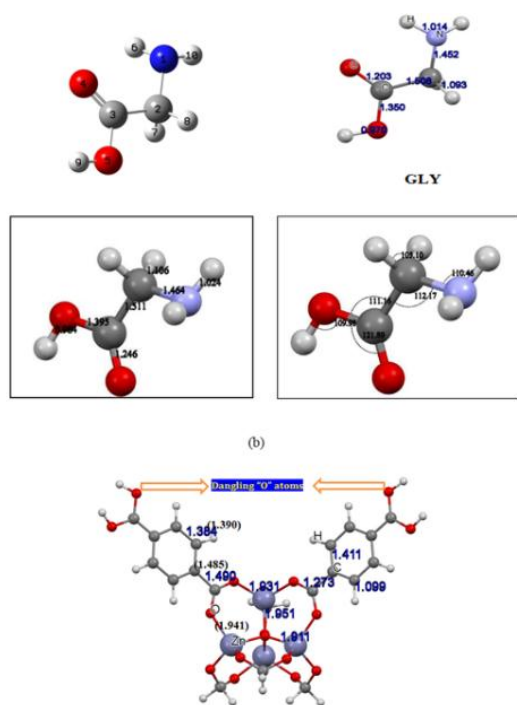


Figure 3. Schematic view of the optimized structure of (a) a tripeptide molecule and (b) energetically favorable configuration of tripeptide/MOF-5 complex.

Conclusions

In this work, interactions of the non-ionic glycine amino acid with the MOF-5 were explored using the state-of-the-art DFT/revPBE-D3 level of theory. Various configurations were selected for the glycine interacting with the MOF skeleton. Our first-principles calculations in the aqueous phase demonstrated that the

glycine was strongly bound to the MOF-5 through a Zn atom on the N/O active sites. The calculated interaction energy and bond lengths provided sufficient evidence to conclude that the interaction process went through a chemisorptions mechanism and the complex was highly stable in terms of interaction energy. Furthermore, the calculated electronic structure and charge density and the results of AIM analysis elucidated the strength of the bonding between the respected amino acid and the MOF-5. The calculated values of hardness and energy gap of the Gly/MOF-5 complex were lower than those of the amino acid, increasing the reactivity of the respective system. The effect of solvent and non-local dispersion interactions (vdW forces) were also evaluated and the results indicated that neither the solvent nor the vdW forces imposed any significant effect on the binding nature of the interacting system. According to the results of optimization based on the DFT-D3 model, it was figured out that the tripeptide glycine was firmly attached, at high interaction energy, to the MOF-5 through its carbonyl and carboxyl active sites. This led us to the conclusion that energy-stable complexes can be obtained by coupling the tripeptide glycine with the MOF-5. Generalizing this conclusion, one may expect stable complexes by attaching similar biological systems (e.g. proteins with active sites provided by carboxyl and carbonyl oxygen and amino nitrogen) to the MOF-5. What we found according to the DFT-D3 model sets the scene for developing novel biomolecule-MOF-5 complexes for a wide variety of applications including nano-scaled drug delivery systems.

Computational method:

Our calculations were performed to investigate the interaction between amino acids and MOF-5 nanostructure based on the DFT method. As the most extensively applied computational technique in the field, the DFT was utilized in this research. Specifically designed for quantum chemistry analysis, ORCA Ver. 3.0.3 [24] was utilized to perform all electron DFT calculations based on revised Perdew–Burke–Ernzerhof (revPBE) functional and generalized gradient approximation (GGA) [25, 26]. For this purpose, optimization and energy calculations were performed using split-valence plus polarization basis set (def2-SVP) for light atoms and triple- ζ plus polarization basis set (def2-TZVP) for metals as per the approach presented by Ahlrichs *et al.* [27-31]. To have the NormalOpt convergence criteria satisfied in ORCA, all structures were subjected to optimization

thoroughly, with the convergence criterion for SCF iterations set to VeryTightSCF to attenuate the noise contaminating the gradient calculations [14, 36]. To take long range dispersion interactions into consideration, a combination of Grimme's atom pair-wise dispersion corrections (3rd version) with Becke–Johnson damping, called D3-BJ, were utilized [32-34]. The impact of the incomplete nature of the basis set in non-covalently bonded systems was attenuated using counterpoise correction [35] to lower the basis set superposition error (BSSE). In the meantime, when it came to covalently bonded systems, the optimized structures were subjected to single-point energy calculations based on the def2-TZVP basis set in an attempt to provide energies near the basis set limit. Interaction energies were evaluated as follows:

$$E_{\text{ads}} = E_{\text{MOF-Gly}} - (E_{\text{MOF}} + E_{\text{Gly}}) - \sigma \text{BSSE} \quad (1)$$

Where $E_{\text{MOF-Gly}}$, E_{MOF} , and E_{Gly} refer to the total energies of the complex, MOF-5, and glycine amino acid/tripeptide conformer, respectively. The proposed method was verified by comparing the evaluated basis sets against the respective experimental data as well as reliable theoretical methods such as MPn and PW6B95, as per reports published elsewhere [22, 36-39]. The quantum theory of atoms in molecules (QTAIM) (also known as atoms-in-molecules (AIM) theory) was utilized to explore and characterize the nature of interactions among the studied complexes. The theoretical basis of the AIM theory has been detailed elsewhere [40–42]. In this work, the AIM analysis was used to explore the interactions between the MOF-5 and selected amino acids. For this aim, the ORCA code was utilized to obtain the wave-function used in the bonding analysis by using the DFT method. For the topological analysis and evaluation of local properties, the Multiwfn program was utilized [43, 44]. According to the AIM theory, a bonding critical point (BCP) appears between two atoms forming a bond. Based on the BCP, the electron density ($\rho(r)$) and the sign of its Laplacian (*i.e.* $\nabla^2\rho(r)$) determine whether the formed bond is covalent or electrostatic. For the $\nabla^2\rho(r) < 0$, the charge is concentrated, characterizing a covalent bond, while depleted charges are associated with $\nabla^2\rho(r) > 0$, indicating a closed-shell (electrostatic) interaction. In the case of shared interactions, the accumulation of electron density can be seen along the line connecting the respective nuclei, while for the closed shell interactions, the accumulation of charges can be observed at the terminal of the interacting

nuclei, with the BCP at the midway of the bond accounting for the depletion of the electron density. The following equation relates the total energy density ($H(r_{\text{BCP}})$) to the Laplacian of the electron density based on Bader's theory [41]:

$$1/4 \nabla^2\rho(r_{\text{BCP}}) = G(r_{\text{BCP}}) + H(r_{\text{BCP}}) \quad (2)$$

Where $G(r_{\text{BCP}})$ indicates the kinetic energy density, which is always a positive value. The molecular properties, including the gap energy (E_g), hardness (η), and softness (s), were also calculated and discussed for the systems under consideration.

References

- [1] Zhang, H.; Nai, J.; Le Yu.; Xiong Wen (David) Lou. *J. Joule.*, **2017**, *1*, 77.
- [2] Wang, C.; Liu, D.; Lin, W. *J. Am Chem Soc.*, **2013**, *135*, 13222.
- [3] Horcajada, P.; Gref, R.; Baati, T. *Chem. Rev.*, **2012**, *112*, 1232.
- [4] Wang, J.; Liu, Y.; Jiang, M.; Li, Y.; Xia, L. *ChemCommun.*, **2018**, *54*, 1004.
- [5] Kitagawa, S.; Kitaura, R.; Noro, S. *Angewandte Chemie.*, **2004**, *43*, 2334.
- [6] Batten, R.; Champness, R.; Chen, M.; Garcia Martinez.; Kitagawa. *J. Pure Appl. Chem.* **2013**, *85*, 1715.
- [7] Jeffrey, R.; Hong-Cai “Joe” Zhou.; Omar M. Yaghi. *Chem. Rev.*, **2012**, *112*, 673.
- [8] Lu, W.; Wei, Z.; Zhi-Y, Gu. *J. RSC Adv.*, **2014**, *148*, 359.
- [9] Imaz, I.; Rubio-Martínez, M.; An, J.; Sole-Font, I.; Rosi, N.L.; MasPOCH, D. *ChemCommun.*, **2011**, *47*, 7287.
- [10] Weber, R.; Bergerhoff, G. *Z. Kristallographie.*, **1991**, *195*, 878.
- [11] Li, J.-R.; Tao, Y.; Yu, Q.; Bu, X.-H.; Sakamoto, H.; Kitagawa, S. *Chem.Eur. J.* **2008**, *14(9)*, 2771.
- [12] Eddaoudi, M.; Kim, J.; Rosi, N.; Vodak, D.; Wachter, J.; O’Keeffe, M.; Yaghi, O. M. *Science.*, **2002**, *295*, 469.
- [13] Qiang, Z.; Yong Yuan, T; Zhu, L ; Liu, Z. *J. Mater. Chem. A.*, **2015**, *3*, 525.
- [14] T. Larijani, H.; Ganji, M. D.; Jahanshahi, M. *J. RSC Adv.*, **2015**, *5*, 92843.
- [15] Pantarotto, D.; Singh, R.; McCarthy, D.; Erhardt, M.; Briand, J. P.; Prato, M.; Kostarelos, K.; Bianco, A. *Angew. Chem.*, **2004**, *116*, 5354.
- [16] Meng, S.; Maragakis, P.; Papaloukas, C.; Kaxiras, E. *Nano Lett.*, **2007**, *7*, 45.

- [17] Willner, I.; Willner, B. *Nano Lett.*, **2010**, *10*, 3805.
- [18] Marshall, R.; Hobday, CL.; Murphie, CF.; Griffin, SL. *J. Mater. Chem. A.*, **2016**, *4*, 6955.
- [19] Zhang JH.; Nong RY.; Xie SM.; Wang BJ.; Ai P.; Yuan LM. *J. Electrophoresis.*, **2017**, *38(19)*, 2513.
- [20] Xu, Z. X., Tan, Y. X., Fu, H. R., Kang, Y., Zhang . *ChemCommun .*, **2015**, *51*, 2565.
- [21] Ahangari, M. G.; Fereidoon, A.; Ganji, M. D. *J Mol Model.*, **2013**, *19*, 3127.
- [22] T. Larijani, H.; Jahanshahi, M.; Ganji, M. D.; M. H. Kiani. *Phys.Chem.Chem.Phys.*, **2017**, *19*, 1896.
- [23] Qin, W.; Li, X.; W Bian, W.; J Fan, X.; J Qi, Y. *Biomaterials.*, **2010**, *31*, 1007.
- [24] Neese, F. *J.WIREs Comput Mol Sci.*, **2012**, *2*, 73.
- [25] Perdew, J.; Burke, K.; Ernzerhof, M. *Phys. Rev. Lett.*, **1996**, *77*, 3865.
- [26] Schäfer, A.; Huber, C.; Ahlrichs. *J. Chem. Phys.*, **1994**, *100*, 5829.
- [27] Baerends, E.; Ellis, D.; Ros, P., 1973, *2*, 41.
- [28] Dunlap , B.I; Connolly, J.; Sabin, J. *J. Chem. Phys.*, **1979**, *71*, 3396.
- [29] Van Alsenoy, C. *J. Comput. Chem.*, 1988, *9*, 620.
- [30] Kendall, R.A.; Fruchtl, H. A.; *Theor Chem Acc.*, **1997**, *97*, 158.
- [31] Eichkorn, K.; Weigend, F.; Treutler, O.; Ahlrichs, R. *Theor Chem Acc.*, **1997**, *97*, 119.
- [32] Grimme, S.; Antony, J.; Ehrlich, S.; Krieg, H. *J. Chem. Phys.*, **2010**, *132*, 154104.
- [33] Becke, AD.; Johnson, ER. *J. Chem. Phys.*, **2005**, *123*, 154101.
- [34] Johnson, ER.; Becke, AD. *J. Chem. Phys.*, **2006**, *124*, 174104.
- [35] Boys, S. F.; Bernardi, FD. *J. Mol. Phys.*, **1970**, *19*, 553.
- [36] Soleymani, E.; Alinezhad, H.; Ganji, M. D.; ajbakhsha, M . *J. Mater. Chem. B*, **2017**, *5*, 6920.
- [37] Alinezhad, H.; Ganji, M. D.; E. Soleymani.; Tajbakhsh, M. *Appl. Surf. Sci.*, **2017**, *422*, 56.
- [38] Moradi, F.; Ganji, M. D.; Sarrafi, Y. *Phys.Chem. Chem. Phys.*, **2017**, *19*, 8388.
- [39] Ganji, M. D.; Mirzaei, Sh.; Dalirandeh, Z. *Sci. Reports.*, **2017**, *7*, 4669.
- [40] Popelier, P.L.A. *Atoms in Molecules. An Introduction*; Pearson Education: Harlow, UK, (**2000**).
- [41] Bader, R.F.W. *Atoms in Molecules. A Quantum Theory*; Oxford Science Publications, Clarendon Press: London, UK, (**1990**).
- [42] Cort'es-Guzman, F.; Bader, R.F.W .*J. Coord. Chem.*, **2005**, *249*, 633.
- [43] Lu, T.; Chen, F. *J. Comp. Chem.*, **2012**, *33*, 580.
- [44] Lu, T.; Chen, F. *J. Mol. Graph.*, **2012**, *38*, 314.
- [45] Rosi, N.L.; Eckert, J.; Eddaoudi, M.; Vodak, David T.; Kim, J.; O'Keefe, M.; Yaghi, O. *Science.*, **2003**, *300*, 1127.
- [46] G. te Velde , F. M.; Bickelhaup, E. J.; Baerends C. F.; Guerra, S. J. A.; van Gisbergen, J. G.; Snijders, T. Ziegler, *J. Comp. Chem.* **2001**, *22*, 931.
- [47] Guerra, C. F. Handgraaf, J-W. Bearends, E. J. F. M. Bickelhaupt, *J. Comp. Chem.* **2004**, *25*, 189.
- [48] Koopmans, T. *Physica*, **1934**, *1*, 104.
- [49] Parr, R. G., Yang, W. *Ann. Rev. Phys. Chem.* **1995**, *46(1)*, 701.
- [50] Parr, R. G.; Pearson, R. G. *J. Am. Chem. Soc.*, **1983**, *105(26)*, 7512.
- [51] Pearson, R. G. *Chemical hardness* (p. 198). New York: Wiley-VCH (**1997**).
- [52] Alinezhad, H.; Darvish Ganji, M.; Soleymani, E.; Tajbakhsh, M. *Appl. Sur. Sci.* **2017**, *422*, 56.
- [53] Rezvani, M.; Darvish Ganji, M.; Jameh-Bozorgi, S. *Appl. Sur. Sci.* **2016**, *360*, 69.
- [54] Darvish Ganji, M. Jameh-Bozorgi, S. Rezvani, M. *Appl. Sur. Sci.* **2016**, *384*, 175.
- [55] Topsakal, M.; Cahangirov, S.; Bekaroglu, E.; Ciraci, S. *Phys. Rev. B.*, **2009**, *80*, 235119.